Journal of Solid State Chemistry **159,** 181–185 (2001)
doi:10.1006/jssc.2001.9148, available online at http://www.idealibrary.com on IDEAL®

Preparation and Characterization of Nanocrystal V_2O_5

Chenmou Zheng,*,[1] Xinmin Zhang,* Zhengping Qiao,* and Deming Lei†

*School of Chemistry and Chemical Engineering, †Department of Physics, Zhongshan University, Guangzhou 510275, People's Republic of China

Received December 1, 2000; in revised form February 26, 2001; accepted March 15, 2001; published online May 11, 2001

Nanocrystal V_2O_5 with granular shape and of various sizes was prepared by oxidative pyrolysis of the single molecular precursor, $(NH_4)_5[(VO)_6(CO_3)_4(OH)_9]\cdot 10H_2O$, at $\leq 630^\circ C$ in a flow of air or oxygen gas. The thermolysis process of the precursor was investigated by TGA/DTGA and DTA in a flow of air. The data of the DTA curve indicate that fine particles of V_2O_5 are easier to crystallize and have a lower melting point. The IR spectra of various size V_2O_5 show that the absorption wavenumbers of the bands decreased gradually and the absorption at $494 \sim 518\,cm^{-1}$ disappeared gradually as the powder sizes decreased, which is attributed to size effect. © 2001 Academic Press

Key Words: **nanocrystal vanadium pentoxide; preparation; crystallization and melting point; IR spectra; size effect.**

1. INTRODUCTION

V_2O_5 is known as an *n*-type semiconductor (1). A great deal of effort has been devoted to the problems of electrical properties such as V_2O_5 ceramics (2), V_2O_5-based materials (3), and cathode active materials used in high-energy batteries (4). V_2O_5 is also an excellent catalyst (5, 6). Ultrafine V_2O_5 powders (> 100 nm) are prepared by heating $V_2O_5\cdot nH_2O$ gels, which are generally produced as follows: (a) decavanadic acid prepared by ion exchange on a resin from sodium metavanadate solution is polymerized over a long period of time (7). (b) $VO(OC_2H_5)_3$ is hydrolyzed using the sol–gel process, which uses uneconomic $VO(OC_2H_5)_3$ (2). Ultrafine V_2O_5 is also produced from a dilute vanadium nitrate solution (8) or a dilute vanadyl sulfate solution (9) using the spray-pyrolysis method. However, this process requires a complex spray pyrolysis reactor. Nanometer-sized V_2O_5 powder (< 100 nm) is synthesized by laser-induced vapor-phase reaction (10), but producing a large amount of the powder using this method is difficult.

In this work, we report a novel convenient method for preparing nanocrystal V_2O_5 powders with granular shape of various sizes by oxidative pyrolysis of the single molecular precursor, $(NH_4)_5[(VO)_6(CO_3)_4(OH)_9]\cdot 10H_2O$, in a flow of air or oxygen gas. The choice of this precursor is based on the following considerations that it is easily synthesized (11) and that nanocrystal V_2O_5 is expected to be easily obtained due to the releasing of a large amount of gases during pyrolysis. Advantages of this approach includes the ability to easily generate nanocrystal V_2O_5 at low production cost and high production rate using commercial V_2O_5 as a starting material (11).

[1] To whom correspondence should be addressed. E-mail: daddy200@sina.com.

2. EXPERIMENTAL SECTION

2.1. Preparation and Pyrolysis of the Precursor

The precursor with particles of size ≤ 2 μm was synthesized using the route (11): $V_2O_5 + HCl + N_2H_4\cdot 2HCl \rightarrow VOCl_2 + NH_4HCO_3 \rightarrow (NH_4)_5[(VO)_6(CO_3)_4(OH)_9]\cdot 10H_2O$. The material was then spread in a quartz boat and a flow of air ($\geq 500^\circ C$) or 99.5% oxygen gas ($< 500^\circ C$) was introduced in the system and then heated to obtain V_2O_5. The purities of the starting material V_2O_5 (c.p.) and the product V_2O_5 were determined by inductively coupled plasma–atomic emission spectroscopy (ICP–AES), respectively. The total impurity content of V_2O_5 (c.p.) amounted to about 1000 at. ppm, with Cr, Sb, and Ga as the main sources of impurity; the total impurity of product V_2O_5 amounted to $50 \sim 350$ at. ppm, showing that the material used in this study was purified in the synthesis process of the precursor-like sol–gel process of $VO(OC_2H_5)_3$ (2).

2.2. Thermoanalysis of Precursor and Characterization of Product V_2O_5

Differential thermal analysis (DTA) and thermogravimetic analysis (TGA/DTGA) of the precursor were completed on a Perkin–Elmer DTA-1700 and a Perkin–Elmer TGS-2, respectively, with a heating rate at $5^\circ C\ min^{-1}$ and an air flow rate of 100 ml min^{-1}. X-ray diffraction (XRD) for V_2O_5 was carried out on a D/max-3A diffractometer using Cu$K\alpha$1 radiation ($\lambda = 0.154050$ nm). The feature micrographs were obtained by transmission

0022-4596/01 $35.00

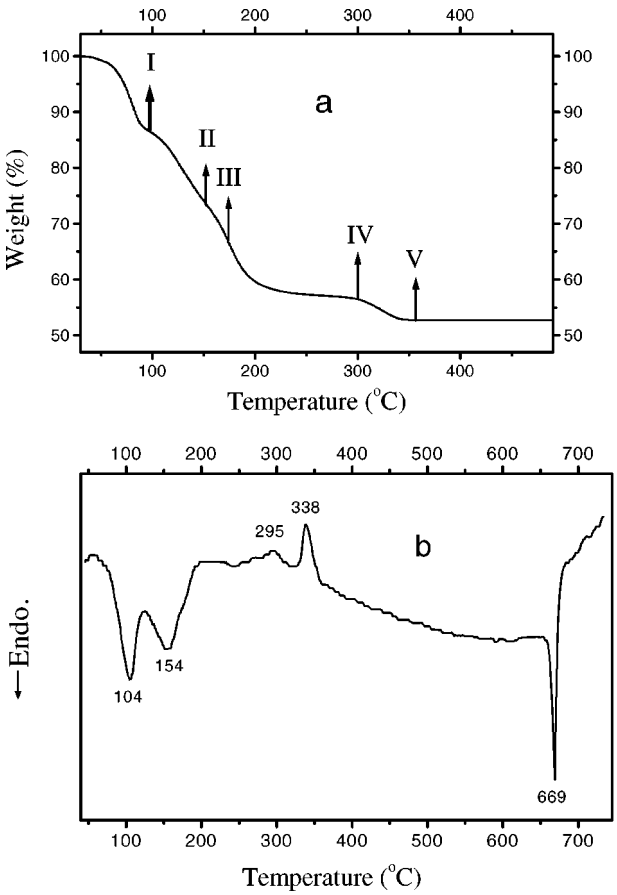

FIG. 1. (a) TGA and (b) DTA curves of thermolysis of the precursor in a flow of air, heating rate at 5°C min^{-1}, air flow rate of 100 ml min^{-1}

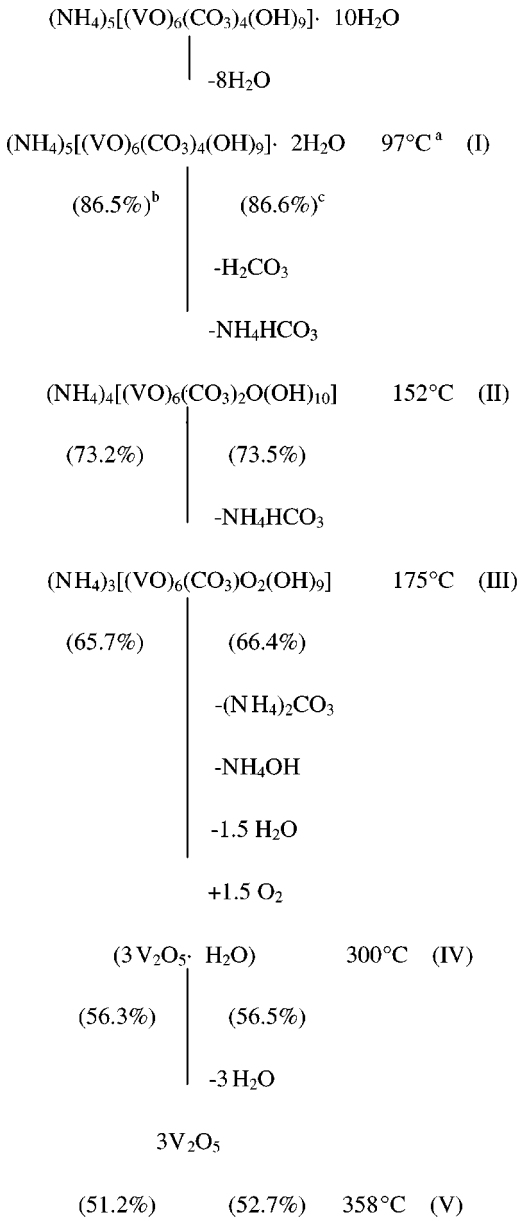

FIG. 2. Schematic representation of the thermolysis process of the precursor: (a) the temperature of a formation of intermediates; (b,c) the calculated and experimental value of residual fractional weight, respectively.

electron microscope (TEM) using a JEM 100-CX-II TEM, in which the samples were dispersed by supersonic pulverizer in water. The IR spectra of the V_2O_5 powders were obtained on a BRUKER EQUINOX 55 spectrometer. The samples were laid in a desiccator with P_2O_5 and quickly pressed in KBr.

3. RESULTS AND DISCUSSION

3.1. Thermoanalysis and Pyrolysis of the Precursor

The thermoanalysis results of the precursor are shown in Fig. 1, and a thermolysis model is displayed in Fig. 2. The TGA data in Fig. 1a indicate that there were four intermediates, i.e., $(NH_4)_5[(VO)_6(CO_3)_4(OH)_9]\cdot 2H_2O$ (I, 97°C), $(NH_4)_4$ $[(VO)_6(CO_3)_2O(OH)_{10}]$ (II, 152°C), $(NH_4)_3[(VO)_6(CO_3)O_2(OH)_9]$ (III, 175°C), and $V_2O_5\cdot H_2O$ (IV, 300°C), as well as the final product V_2O_5 (V, 358°C) in the oxidative pyrolysis process. In comparison with the intermediates obtained from thermolysis of the precursor in a flow of nitrogen gas, intermediate I is the same and intermediates II and III are also the same (12). There are two endothermic peaks at 104 and 154°C on the DTA curve in Fig. 1b. The former is due to the thermolysis effect of the formation of I, and the latter is due to that of the formation of II and III. The exothermic peak at 295°C is due to the oxidation of the intermediate III during a later period of its thermolysis. However, an endothermic peak of dehydration of $V_2O_5\cdot H_2O$ corresponding to the temperature range from 280 to 358°C on the TGA curve in Fig. 1a is not observed on the DTA curve, which futher confirms the

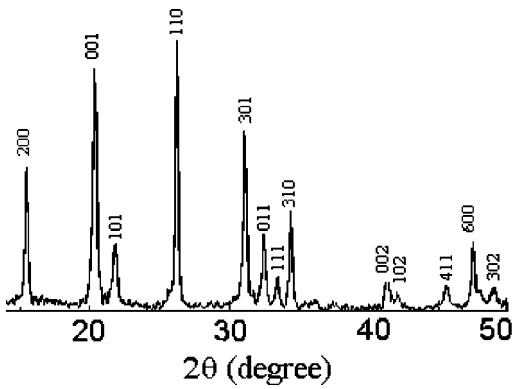

FIG. 3. XRD patterns of V_2O_5 obtained at 290°C for 72 h.

above-mentioned explanation. Further investigation on the DTA curve demonstrates that V^{4+} does not significantly oxidize at < 240°C. This is very different from $VO(OH)_2$, which oxidizes fast in air at room temperature. In other words, the V^{4+} ions in ammonium vanadyl carbonato hydroxide such as the precursor and the intermediates I, II, and III are considerably stable to oxygen. In fact, we found that the precursor did not oxidize after being exposed to air for even longer periods of time (13). Another exothermic peak at 338°C is due to the crystallization of V_2O_5. In comparison with the thermoanalysis data of $V_2O_5 \cdot nH_2O$ gels, the top peak at 338°C is lower than at 350°C (14), which indicates that the fine V_2O_5 powders are easily crystallized. The above result shows that the stage of the dehydration and the crystallization of the material was believed to occur simultaneously, similar to that in the thermolysis of $V_2O_5 \cdot nH_2O$ gels (2, 15). The sharp endothermic peak at 669°C on the DTA curve is due to the melting effect of the product V_2O_5. The melting point (669°C) of fine V_2O_5 powder is lower than that of bulk particle of V_2O_5 (680 or 676°C) (2, 14, 16), which also indicates that fine particles of V_2O_5 are easier to melt. The above results are due to size effect.

Pyrolysis of the precursor was carried out at various temperatures to generate various sizes of V_2O_5 powder, in order to observe the properties of the obtained products. To accelerate oxidation of V^{4+}, oxygen gas was introduced in the system instead of air at < 500°C. Even so, the complete oxidation of V^{4+} required 72 h at 290°C, and the product obtained is still crystalline V_2O_5; the XRD pattern is shown in Fig. 3. Attempts to obtain $V_2O_5 \cdot xH_2O$ or amorphous V_2O_5 did not succeed by pyrolysis of the precursor at lower temperature, indicating that the stage of the oxidation, the dehydration, and the crystallization of the material occurred simultaneously under the conditions of a larger amount of the precursor and a lower temperature.

TABLE 1
IR Spectra of Various Size V_2O_5 (cm^{-1})

Pyrolysis condition	Size (nm)	v_1	v_2	v_3	v_4	v_5
630°C, 1 h	< 400	1020	838	634	518	481
600°C, 0.5 h	< 200	1019	836	634	512	481
500°C, 1 h	< 110	1019	831	632	512	479
500°C, 0.5 h	< 80	1020	831	629	494	479
330°C, 6 h	< 60	1018	830	629		478
310°C, 24 h	< 40	1017	828	628		476

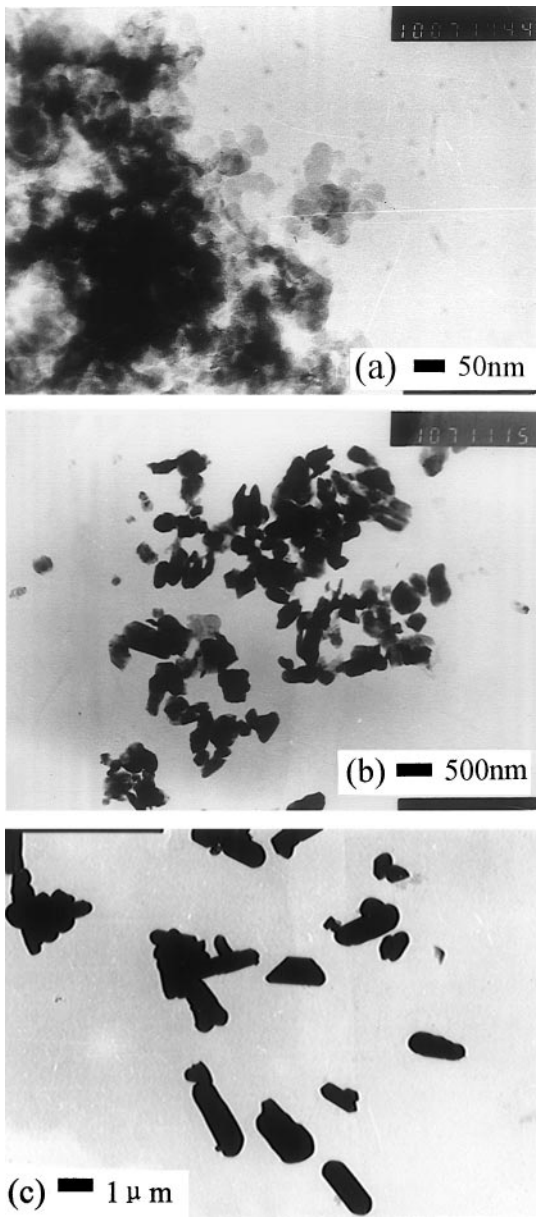

FIG. 4. TEM micrographs of V_2O_5 powders obtained at (a) 310°C for 24 h, (b) 630°C for 1 h, (c) 660°C for 1 h.

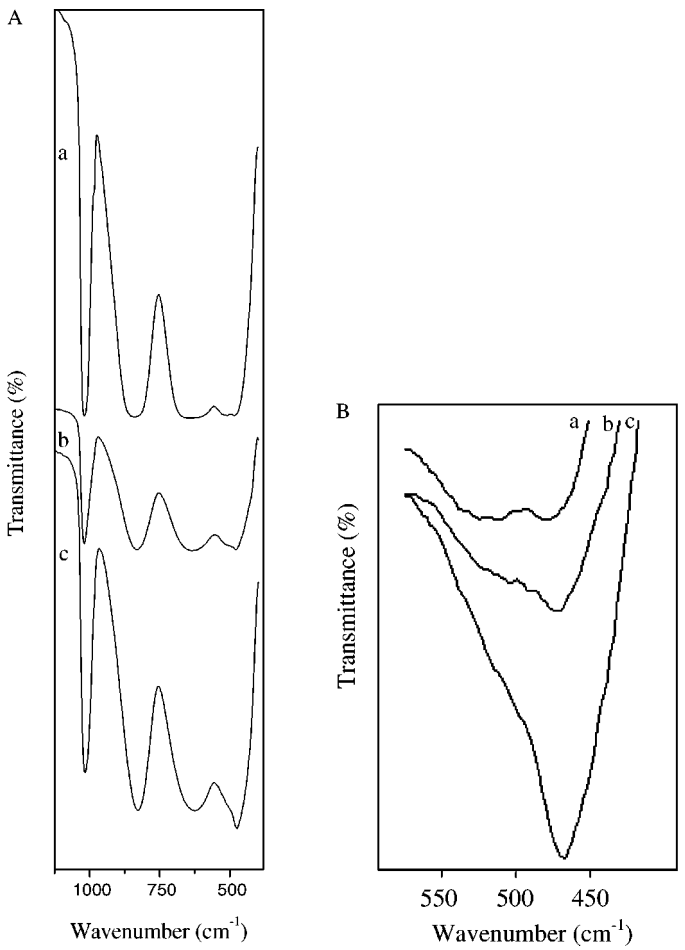

FIG. 5. (A) IR spectrograms of V_2O_5: (a) 630°C, 1 h; (b) 500°C, 1 h; (c) 310°C, 24 h. (B) IR spectrograms of V_2O_5 with an extended zone of $420 \sim 560\ cm^{-1}$

3.2. *Morphology of V_2O_5 products*

The sizes of the products obtained under the conditions of various pyrolysis are listed in Table 1, and the typical micrographs of as-prepared V_2O_5 powders are shown in Fig. 4. Figure 4 and Table 1 show that the sizes of V_2O_5 particles obtained at 310°C for 24 h, 500°C for 1 h, and 630°C for 1 h were < 40, < 110, and < 400 nm, respectively. Only strip-like particles ~ 2.4 μm long and ~ 0.8 μm wide at 660°C near the melting point of V_2O_5 for 1 h grew from the procedure. Honma *et al.* (2) reported that the sizes of V_2O_5 particles with ~ 350 nm and the strip-like shape particles with ~ 4 μm long and ~ 1 μm wide were, respectively, obtained at 500 and 630°C for 1 h by heating $V_2O_5 \cdot 2.07H_2O$ gel. Obviously, V_2O_5 with finer size and granular shape is easily prepared using our method reported in this paper, which may be attributed to the release of a large amount of gases and to the oxidation during the pyrolysis of the precursor, which caused strong splitting and atomizing of the particles. Moreover, the gases absorbed on the powder also inhibited the particles from sintering and further growing. In fact, NH_3 was detected from the sample obtained at 500°C.

3.3. *IR Spectra of Various Size V_2O_5*

The IR data of various size V_2O_5 are also listed in Table 1 and typical IR spectra are shown in Fig. 5. The results in Fig. 5A show that there were two modifications of IR spectra from bulk crystals to fine crystals: the absorption wavenumbers are lowered gradually, the absorption at $494 \sim 518\ cm^{-1}$ disappeared gradually. This phenomenon was observed in the amorphism (17, 18) and gels (19) of V_2O_5, also observed in amorphous and nano-crystalline VO_2 powder (11). The size effect of crystalline V_2O_5 (19, 20) can be associated with the huge surface of material. With a decrease of particle size, crystal boundaries and surface area of material increase drastically. Since the V=O and V–O bond on the crystal surface is not strictly limited by the crystal lattice, the V=O or V–O distance gets longer and the bond angles on the surface are nonuniform, thus resulting in the absorption wavenumber decrease. Moreover, the difference between δ (VO) at $494 \sim 518$ and $476 \sim 481\ cm^{-1}$ on the surface decreases and degenerates finally, resulting in that the absorption at $494 \sim 518\ cm^{-1}$ disappeared and the absorption strength at $476 \sim 481\ cm^{-1}$ increased as shown in Fig. 5B.

ACKNOWLEDGMENT

This work was supported by the Natural Science Foundation (No. 970168) of Guangdong Province of China.

REFERENCES

1. W. D. Kingery, H. K. Bowen, and D. R. Uhlmanm, *in* "Introduction to Ceramics" (2nd ed.), p. 890. Wiley, New York, 1976.
2. K. Honma, M. Yoshinaka, K. Hirota, and O.Yamaguchi, *Mater. Res. Bull.* **31,** 531 (1996).
3. R. Iordanova, Y. Dimitriev, V. Dimitrov, S. Kassabov, and D. Klissurski, *J. Non-Cryst. Solids* **204,** 141 (1996).
4. X. Bi, S. Kumar, J. T. Gardner, and N. Kambe, **WO,** 04,441 (1999).
5. F. P. Miquel and L. J. Katz, *in* "Advances in Catalytic Nanostructural Materials" (R. W. Moser, Ed.), p. 515. Academic Press, San Diego, 1996.
6. F. Arena, F. Frusteri, A. Parmaliana, G. Martra, and S. Coluccia, *Stud. Surf. Sci. Catal.* **119,** 665 (1998).
7. J. Lemerle, L. Nejem, and J. Lefebvre, *J. Chem. Res.* (*M*), 5301 (1978).
8. Y. Xiong, S. W. Lyons, T. T. Koda, and S. E. Pratsin, *J. Am. Ceram. Soc.* **78,** 2490 (1995).
9. S. A. Lanton and E. A. Theby, *J. Am. Ceram. Soc.* **78,** 104 (1995).

10. O. Toshiyuki, I. Yasuhiro, and R. K. Kenkyu, *J. Photopolym. Sci. Technol.* **10,** 211 (1997).
11. C. Zheng, X. Zhang, J. Zhang, and K. Liao, *J. Solid State Chem.* **156,** 274 (2001).
12. C. Zheng, J. Zhang, G. Luo, J. Ye, and M. Wu, *J. Mater. Sci.* **35,** 3425 (2000).
13. T. C. W. Mak, P. Li, C. Zheng, and K. Huang, *J. Chem. Soc., Chem. Commun.* **21,** 1597 (1986).
14. P. Aldebert, N. Baffier, N. Gharbi, and J. Livage, *Mater. Res. Bull.* **16,** 669 (1981).
15. N. Soga and M. Senna, *J. Solid State Chem.* **107,** 159 (1993).
16. H. Oppermann, W. Reichelt, U. Gerlach, E. Wole, W. Brückner, W. Moldenhauer, and H. Wich, *Phys. Status Solidi A* **28,** 439 (1975).
17. W. E. Steger, H. Landmesser, U. Boettcher, and E. Schubert, *J. Mol. Struct.* **217,** 341 (1990).
18. C. Sanchez, J. Livage, and G. Lucazeau, *J. Raman Spectrosc.* **12,** 68 (1982).
19. L. Abello, E. Husson, Y. Repelin, and G. Lucazeau, *J. Solid State Chem.* **56,** 379 (1985).
20. L. Abello, E. Husson, Y. Repelin, and G. Lucazeau, *Spectrochim. Acta Part A* **39,** 641 (1983).